bourne for granting sabbatical leave (T.A.O.). We wish to thank R. N. R. Mulford of Los Alamos National Laboratory for providing the samples of Np metal used in this work.

This work was supported by the Division of Chemical Sciences, Office of Basic Energy Sciences, U.S. Department of Energy, under Contract No. W-7405-Eng-48.

Registry No. AHF, 7664-39-3; U(III), 22578-81-0; U(IV), 16089-60-4; U(V), 22537-60-6; U(VI), 22541-40-8; Np(III), 21377-65-1; Np(IV), 22578-82-1; Np(V), 22537-61-7; Np(VI), 22541-66-8; UF_2^{2+}, 18785-29-0.

Contribution from the Department of Chemistry, Michigan State University, East Lansing, Michigan 48824

ESR Studies of Some Oxotetrahalo Complexes of Vanadium(IV) and Molybdenum(V)

K. K. SUNIL and M. T. ROGERS*

Received October 24, 1980

ESR spectra of $[VOF_4]^{2-}$ and $[MoOF_4]^-$ have been studied in single crystals of $(NH_4)_2SbF_5$ and spectra of $[MoOCl_4]^-$ in single crystals of $(NH_4)_2SbCl_5$. The spin-Hamiltonian parameters of these pentacoordinated complexes have been obtained and compared with those for the corresponding hexacoordinated species. Molecular orbital parameters for the penta- and hexacoordinated species obtained from experimental **g**- and **A**-tensor components have been compared with values calculated by the MS-SCF-Xα method.

Introduction

The transition-metal oxohalo complexes of the type $[MOX_5]^{m-}$, where M = V, Nb, Cr, Mo, and W and X = F, Cl, Br, and I, have been the subject of detailed ESR studies.[1-20] The **g**, metal hyperfine, and ligand hyperfine tensors have been used to investigate the nature of bonding in these compounds. On the other hand, very little work has been done on the corresponding pentacoordinated oxohalo complexes.[21,22] Since ESR spectroscopy provides a very sensitive probe for the detection and measurement of the effects of small changes in bonding, we have undertaken a fairly detailed study of the single-crystal ESR spectra of $[VOF_4]^{2-}$, $[MoOF_4]^-$, and $[MoOCl_4]^-$ in the hope of getting a better understanding of the differences in the bonding between the penta- and hexacoordinated transition-metal oxohalo complexes.

The pentacoordinated transition-metal complexes form a class of compounds of considerable interest with the structures possessing a diversity of forms between the two limiting symmetries of trigonal bipyramidal (D_{3h} symmetry) and square pyramidal (C_{4v} symmetry).[22-24] The energy barrier between these two structures is predicted[25] to be small for species with five equivalent ligands, and examples are observed to occur in both symmetry classes.[26,27] On the other hand, complexes having an axial ligand different from the other four tend to form square-pyramidal complexes.[24] The pentacoordinated oxohalo complexes under investigation here fall in the latter category.

ESR studies of VO^{2+} and Cr^{3+} in $(NH_4)_2SbCl_5$[21] and Fe^{3+} in $(NH_4)_2SbF_5$[28] have been found to provide pentacoordinated species $[VOCl_4]^{2-}$, $[CrCl_5]^{2-}$, and $[FeF_5]^{2-}$, respectively, while for Cr^{3+} in K_2SbF_5 the species which predominates[29] is trigonally-distorted $[CrF_6]^{3-}$. ESR spectra of $[MoOCl_4]^-$ have been studied in solution as well as in a diluted single crystal of $[AsPh_4][NbOCl_4]$.[32] We have carried out the ESR studies of the fluoro complexes of VO^{2+} and MoO^{3+} in ammonium

(1) N. S. Garif'yanov, *Dokl. Akad. Nauk SSSR*, **155**, 385 (1954).
(2) K. D. Bowers and J. Owen, *Rep. Prog. Phys.*, **18**, 304 (1955).
(3) N. S. Garif'yanov and V. N. Fedotov, *Zh. Strukt. Khim.*, **3**, 711 (1962).
(4) N. F. Garif'yanov, V. N. Fedotov, and N. S. Kucheryaenko, *Izv. Akad. Nauk SSSR, Ser. Khim.*, **4**, 743 (1964); *Bull. Acad. Sci. USSR, Div. Chem. Sci. (Engl. Transl.)*, 589 (1964).
(5) N. S. Garif'yanov, *Dokl. Akad. Nauk. SSSR*, **135**, 385 (1964).
(6) K. DeArmond, B. B. Garrett, and H. S. Gutowsky, *J. Chem. Phys.*, **42**, 1019 (1965).
(7) D. I. Gyabchikov, I. N. Marov, Y. N. Dubrov, V. K. Belyaeva, and D. N. Ermakov, *Dokl. Akad. Nauk SSSR*, **169**, 1107 (1966); *Dokl. Phys. Chem. (Engl. Transl.)*, **169**, 795 (1966).
(8) J. T. C. Van Kemenade, J. L. Verbeek, and P. F. Cornaz, *Recl. Trav. Chim., Pays-Bas*, **85**, 629 (1966).
(9) H. Kon and N. H. Sharpless, *J. Phys. Chem.*, **70**, 105 (1966).
(10) M. M. Abraham, J. P. Abriata, M. E. Foglio, and E. Pasquini, *J. Chem. Phys.*, **45**, 2069 (1966).
(11) J. L. Verbeek and P. F. Cornaz, *Recl. Trav. Chim. Pays-Bas*, **86**, 209 (1967).
(12) J. L. Verbeek and A. T. Vink, *Recl. Trav. Chim. Pays-Bas*, **86**, 913 (1967).
(13) R. D. Downing and J. F. Gibson, *J. Chem. Soc. A*, **1**, 655 (1967).
(14) J. L. Verbeek, "Ligand Hyperfine Structure in the ESR Spectra of the Ions $[CrOF_5]^{2-}$ and $[MoOF_5]^{2-}$", Thesis, Eindhoven, 1968.
(15) P. T. Manoharan and M. T. Rogers, *J. Chem. Phys.*, **49**, 5510 (1968).
(16) P. T. Manoharan and M. T. Rogers, *J. Chem. Phys.*, **49**, 3912 (1968).
(17) J. T. C. Van Kemenade, "Ligand Hyperfine Interactions in Oxyhalides of Pentavalent Chromium, Molybdenum and Tungsten", Thesis, Eindhoven, 1970.
(18) J. R. Shock and M. T. Rogers, *J. Chem. Phys.*, **58**, 3356 (1973).
(19) L. A. Dalton, R. D. Bereman, and C. H. Brubaker, Jr., *Inorg. Chem.*, **8**, 2477 (1969).
(20) C. D. Garner, L. H. Hill, F. E. Mabbs, D. L. McFadden, and A. T. McPhail, *J. Chem. Soc., Dalton Trans.*, 853 (1977).
(21) J. M. Flowers, J. C. Hempel, W. E. Hatfield, and H. H. Dearman, *J. Chem. Phys.*, **58**, 1479 (1973).
(22) E. L. Muetterties and R. A. Schunn, *Q. Rev.*, **20**, 245 (1966).
(23) C. Furlani, *Coord. Chem. Rev.*, **3**, 141 (1968).
(24) J. A. Ibers, *Annu. Rev. Phys. Chem.*, **16**, 380 (1965).
(25) J. Zemann, *Z. Anorg. Allgem. Chem.*, **324**, 241 (1963).
(26) (a) M. Mari, Y. Saito, and T. Watanabe, *Bull. Chem. Soc. Jpn.*, **34**, 295 (1961); (b) N. K. Raymond, D. V. Meek, and J. A. Ibers, *Inorg. Chem.*, **7**, 1111 (1968).
(27) (a) J. J. Alexander and H. B. Gray, *J. Am. Chem. Soc.*, **89**, 3356 (1967); (b) K. G. Caulton, *Inorg. Chem.*, **7**, 392 (1968).
(28) C. J. Radnell, J. R. Pilbrow, S. Subramanian, and M. T. Rogers, *J. Chem. Phys.*, **62**, 4948 (1975).
(29) J. C. Hempel, D. Klassen, W. E. Hatfield, and H. H. Dearman, *J. Chem. Phys.*, **58**, 1487 (1973).

0020-1669/81/1320-3283$01.25/0

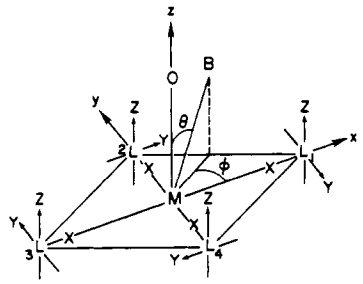

Figure 1. Coordinate axes for description of $[MOL_4]^{m-}$ complexes.

pentafluoroantimonate(III) and the chloro complex of MoO^{3+} in ammonium pentachloroantimonate(III). The ligand hyperfine interactions have been observed for the fluoro complexes at room temperature and the chloro complex at low temperature. We have used the results from our earlier SCF–MS–Xα studies on this class of compounds[37] to interpret the observed **g** and metal hyperfine interaction tensors.

Experimental Section

Ammonium pentafluoroantimonate(III) was made by evaporating a solution of 3 mol of NH_4F and 1 mol of SbF_3 in distilled water. Ammonium pentachloroantimonate(III) was made by evaporation of a solution containing $SbCl_3$ and NH_4Cl in the molar ratio 3:4 in dilute hydrochloric acid.[30] The single crystals of $(NH_4)_2SbF_5$ containing about 1% by weight of VO^{2+} were obtained by slow evaporation of a solution of $(NH_4)_2SbF_5$ and NH_4F in the molar ratio of 1:1 with about 1–2% by weight of $VOSO_4 \cdot 7H_2O$. The single crystals of $(NH_4)_2SbF_5$ containing $[MoOF_4]^-$ were made by dissolving $(NH_4)_2SbF_5$ and NH_4F in water in mole proportion of 1:1, adding a solution of ammonium molybdate in hydrofluoric acid reduced with metallic tin, and allowing the solution to evaporate slowly. The single crystals of $(NH_4)_2SbCl_5$ containing $[MoOCl_4]^-$ were made by dissolving $SbCl_3$ and NH_4Cl in dilute hydrochloric acid in the molar ratio of 3:4, adding a solution of ammonium molybdate in hydrochloric acid, reducing with metallic tin, and allowing the solution to evaporate slowly.

ESR spectra were recorded for the single crystals with use of a Varian E-4 X-band spectrometer. The angular variation of the spectra of each system was obtained by recording the spectra at room temperature for every 10° rotation about three orthogonal axes; in the case of orthorhombic $(NH_4)_2SbF_5$ these were the *a*, *b*, and *c* axes while for monoclinic $(NH_4)_2SbCl_5$ they were the *a*, *b*, and *c** axes. The powder measurements were made with use of powdered samples of the single crystals.

ESR Results

VO^{2+} and MoO^{3+} in $(NH_4)_2SbF_5$. The structure of the orthorhombic host has been reported[31] and each antimony ion is found to be at the center of a distorted octahedron with fluoride ions at five of the vertices and the sterically active lone pair associated with Sb(III) at the sixth. The Sb–F_{ax} direction is parallel to the *b* axis of the crystal and the antimony ion is displaced 0.382 Å from the center of the square formed by the four equatorial fluorides in the direction of the lone pair; Sb–F_{ax} = 1.916 Å and Sb–F_{eq} = 2.075 Å. Two classes of antimony site related by a center of inversion, and magnetically equivalent, are defined in this way.

The vanadyl (VO^{2+}) and molybdenyl (MoO^{3+}) ions can replace either Sb^{3+} or $[Sb–F]^{2+}$ of the $[SbF_5]^{2-}$ ions in $(NH_4)_2SbF_5$ to form either the hexa- or the pentacoordinated complex, or a mixture of both. The ESR spectra of the single crystals of both the systems, VO^{2+} in $(NH_4)_2SbF_5$ and MoO^{3+} in $(NH_4)_2SbF_5$, show intense resonances associated with only one site of a magnetic species. Spectra taken with the magnetic field in the *ac* plane are independent of rotation angle in each case so the paramagnetic ions must have axial symmetry with the V–O or Mo–O direction either parallel to *b* or directed on the surface of a cone making a fixed angle with the *b* axis. These results are consistent with either $[MOF_4]^-$ or $[MOF_5]^{2-}$ (M = V or Mo) as the paramagnetic species.

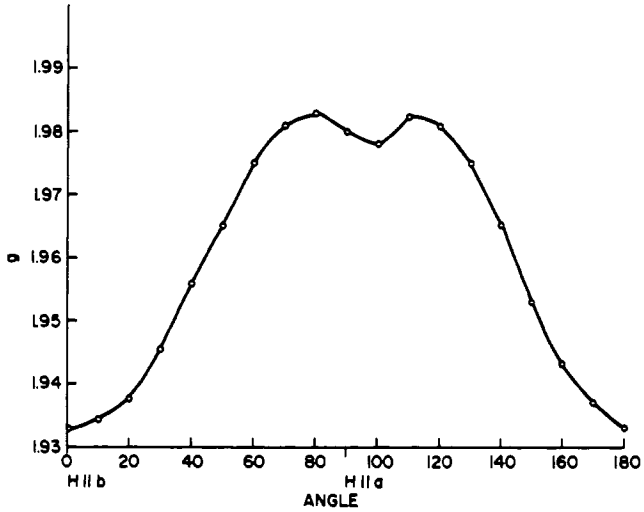

Figure 2. Plot of experimental *g* values vs. orientation of the magnetic field in the *bc* plane for $(NH_4)_2SbF_5$:VO^{2+}.

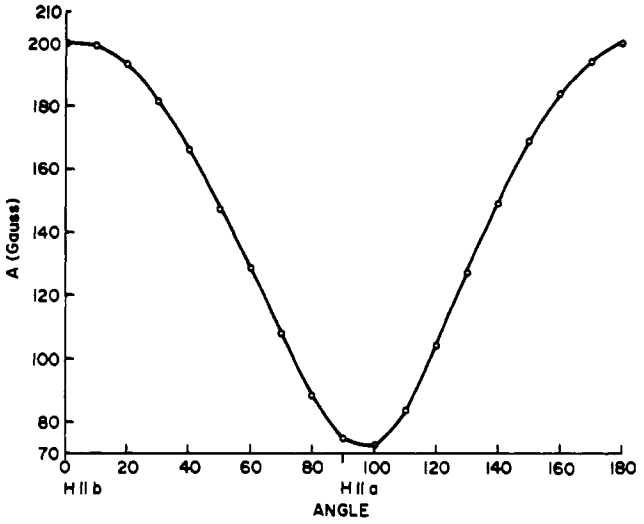

Figure 3. Plot of experimental metal hyperfine splitting values [*A* (G)] vs. orientation of the magnetic field in the *bc* plane for $(NH_4)_2SbF_5$:VO^{2+}.

For analysis of the data, the sets of coordinates shown in Figure 1 were chosen. The **g** and $\mathbf{A}^M$ tensors originate at the metal nuclei with the *z* axis chosen along the M–O bond and the *x* and *y* axes in the equatorial plane formed by the four halide ligands. The origin for each halogen hyperfine tensor $\mathbf{A}^X$ is the halogen atom with the *Z* axis parallel to M–O, the *X* axis along the M–X direction, and the *Y* axis chosen to form an orthogonal, right-handed coordinate system.

The electronic Zeeman and metal hyperfine tensors then obey the relationships

$$g = (g_z^2 \cos^2\theta + g_x^2 \sin^2\theta \cos^2\phi + g_y^2 \sin^2\theta \sin^2\phi)^{1/2} \quad (1)$$

$$gA^M = (A_z^2 g_z^2 \cos^2\theta + A_x^2 g_x^2 \sin^2\theta \cos^2\phi + A_y^2 g_y^2 \sin^2\theta \sin^2\phi)^{1/2} \quad (2)$$

where the angles θ and ϕ relate the external magnetic field vector B_0 to the *z* and *x* axes, respectively (Figure 1). The ESR spectrum for $\theta = 0°$ corresponds to g_z and A_z, that for $\theta = 90°$ and $\phi = 0°$ corresponds to g_x and A_x, and that for $\theta = 90°$ and $\phi = 90°$ corresponds to g_y and A_y. In the case of both VO^{2+} and MoO^{3+} in $(NH_4)_2SbF_5$, it was found that

(30) M. Edstrand, M. Inge, and N. Ingri, *Acta Chem. Scand.*, **9**, 122 (1955).
(31) R. R. Ryan and D. T. Gomer, *Inorg. Chem.*, **11**, 2322 (1972).

Table I. Single-Crystal ESR Parameters of $[MOX_4]^-$ Ions

rotation axis	$g_\parallel$	$g_\perp$	$A_\parallel$, G	$A_\perp$, G
		$[VOF_4]^-$		
a	1.9318	1.9718	−199.61	−74.36
b		1.9728		−72.95
c	1.9325	1.9742	−198.41	−73.11
		$[MoOF_4]^-$		
a	1.8948	1.9253	95.5	
b		1.9256		
c	1.8945	1.9254	95.5	
		$[MoOCl_4]^-$		
	g_{zz} 1.9650[a]	g_{xx} 1.9451	83.19	37.75
		g_{yy} 1.9474		

[a] Values of the principal components of the g tensor were determined with use of Schonland's procedure.

$g_x = g_y$ and $A_x = A_y$, since the spectra are independent of the orientation of the magnetic field in the *ac* plane.

$[VOF_4]^-$ in $(NH_4)_2SbF_5$. Experimental values of g and A^V are plotted vs. the orientation of the magnetic field in the *bc* plane in Figures 2 and 3, respectively. Plots for the *ab* plane are very similar. Values of $g_\parallel$, $g_\perp$, $A_\parallel$, and $A_\perp$ were determined from the measured magnetic field values for the various m_I transitions by a least-squares fitting procedure using eq 3–5,

$$B_0 = B(m_I) + A_\parallel m_I + A_\perp{}^2 \frac{[I(I+1) - m_I{}^2]}{2B(m_I)} \quad (\theta = 0°) \quad (3)$$

$$B_0 = B(m_I) + A_\perp m_I + (A_\parallel{}^2 + A_\perp{}^2)\frac{[I(I+1) - m_I{}^2]}{4B(m_I)} \quad (\theta = 90°) \quad (4)$$

$$B_0 = h\nu/g\beta \quad (5)$$

which are correct to second order. The values of $g_\parallel$, $g_\perp$, $A_\parallel$, and $A_\perp$ determined in this way from angular variation studies in *ab* and *bc* planes are given in Table I, along with the values of $g_\perp$ and $A_\perp$ determined from *b*-axis rotation studies. The spin-Hamiltonian parameters determined from different planes agree within experimental error.

We have observed fluorine hyperfine interaction at room temperature. When the applied magnetic field is along the crystal *b* axis, each of the vanadium hyperfine lines is split into five lines with a separation of 10 G and intensity ratios of approximately 1:4:6:4:1. The fluorine hyperfine interaction was not observed at any other orientation of the crystal with respect to the applied magnetic field at room temperature. We have assigned the observed ESR spectra to the species $[VOF_4]^{2-}$ on the basis of the observed fluorine hyperfine interaction and the fact that one should have observed 10 fluorine hyperfine lines had the species been $[VOF_5]^{3-}$.[16]

The ESR spectra at low temperatures were too complex to analyze, as we could not follow the angular variations of the many different sets of vanadium hyperfine lines that appear at low temperatures.

The analysis of the ESR spectra of the powder sample (Figure 4a) gave spin-Hamiltonian parameter values close to those obtained from the single-crystal studies. The powder spectrum was simulated with use of the spin-Hamiltonian parameter values obtained from single-crystal studies (Figure 4b).

$[MoOF_4]^-$ in $(NH_4)_2SbF_5$. The ESR spectra were fairly well resolved at room temperature, but molybdenum hyperfine lines could be identified only at certain orientations of the magnetic field as a result of the large fluorine hyperfine interaction.

Plots of g vs. orientation of the magnetic field in the *bc* and *ab* planes were made. These were smooth curves with minima for $H \| b$; however, in the *bc* plane g remains constant from θ = 80° to θ = 100° so it was necessary to determine $g_\parallel$ and $g_\perp$ by fitting the experimental g^2 values to eq 6 where θ is the angle the applied magnetic field makes with the crystal *b* axis. With use of the α, β, and γ values determined by the least-squares procedure, g^2 values were computed for all angles and were found to have the minimum at θ = 0° and the maximum at θ = 90° corresponding to $g_\parallel$ and $g_\perp$, respectively. The same procedure was carried out for data in the *ab* plane, and the minimum and maximum in g^2 were found to occur again at θ = 0° and θ = 90°. The $g_\parallel$ and $g_\perp$ values so obtained from rotation studies in the two different planes agree within experimental error and are given in Table I. The g value for rotation about the crystal *b* axis was found to be invariant to the rotation angle and is equal to the $g_\perp$ value determined from data for the *bc* and *ab* planes (Table I). For θ = 0° the molybdenum hyperfine interaction could be measured in both the *ab* and *bc* planes and was found to be 95.5 G. This value was assigned to $A_\parallel$. The $A_\perp$ value could not be measured from the single-crystal studies as very intense fluorine hyperfine lines mask the relatively weak molybdenum hyperfine lines.

$$g^2 = \alpha + \beta \cos 2\theta + \gamma \sin 2\theta \quad (6)$$

For θ = 0° and ϕ = 0°, no fluorine hyperfine interaction was observed (Figure 5a), thus indicating that $A_z(^{19}F)$ was smaller than the line width of the spectrum. For θ = 90° and ϕ = 0° or 90° the fluorine hyperfine structure on the molybdenum I = 0 line consists of a nine-line pattern (Figure 5b). For the case $A_x(^{19}F) \neq A_y(^{19}F) \neq 0$ one expects nine fluorine hyperfine lines with relative intensity ratios 1:2:1:2:4:2:1:2:1, which is approximately what was observed (Figure 5b). From these data $A_x(^{19}F)$ and $A_y(^{19}F)$ were assigned the values −15 and 55 G, respectively.

The ESR spectrum of the powder sample was not resolved well enough to do a complete analysis. The spectrum could not be analyzed by simulation as the simulation program available does not properly take into account the ligand hyperfine interactions.

$[MoOCl_4]^-$ in $(NH_4)_2SbCl_5$. Ammonium pentachloroantimonate forms monoclinic crystals with the *b* axis coinciding

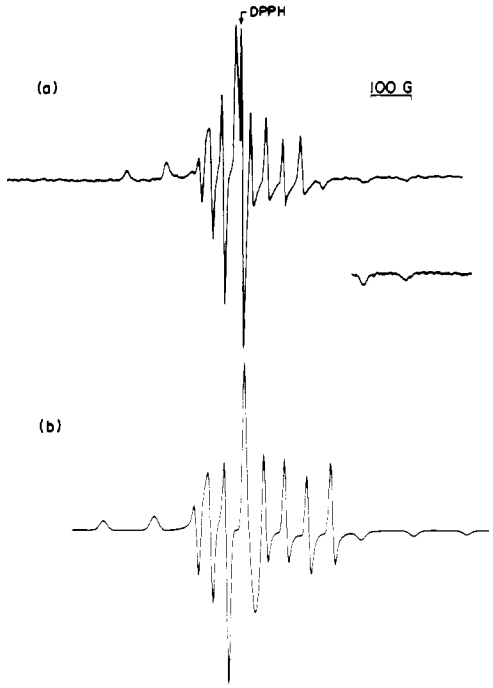

Figure 4. (a) X-Band ESR spectrum of a powder sample of $(NH_4)_2SbF_5$:VO^{2+} at room temperature. (b) Same spectrum simulated with use of the single-crystal spin-Hamiltonian parameters of Table I.

Table II. Molecular Orbital Coefficients for Vanadyl and Molybdenyl Complexes

complex	exptl			SCF-MS-Xα			ref
	β_2	β_1	ϵ	β_2	β_1	ϵ	
$[VOF_4]^{2-}$				0.9565	0.8702	0.8967	this work
$[VOCl_4]^{2-}$	0.98	0.995	1.007	0.9585	0.8340	0.8832	21
$[VOF_5]^{3-}$	0.957[a]	<1.0	<1.0	0.9579	0.8724	0.9050	15
$[VOCl_5]^{3-}$	<1.0	<1.0	0.992	0.9595	0.8371	0.8895	6
$[MoOF_4]^-$				0.9217	0.8075	0.8489	this work
$[MoOCl_4]^-$				0.9055	0.7629	0.8268	this work
$[MoOF_5]^{2-}$	0.956[b]	0.891	0.960	0.9174	0.7856	0.8712	16
$[MoOCl_5]^{2-}$	0.905	0.754	0.901	0.8902	0.7574	0.8488	16

[a] The value $\beta_2 = 0.969$ is obtained from the experimental ligand hyperfine splitting tensor. [b] The value $\beta_2 = 0.83$ was reported[17] with use of the experimental ligand hyperfine splitting tensor.

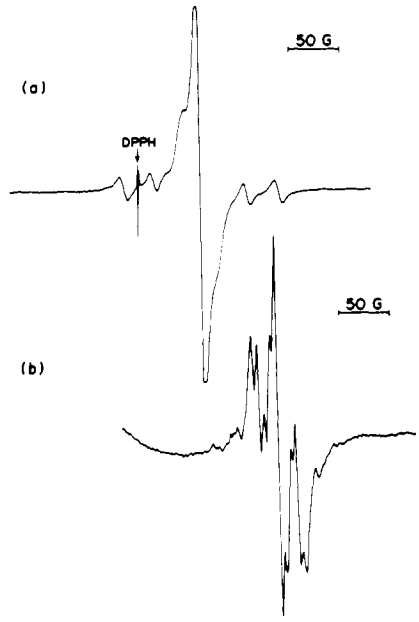

Figure 5. (a) X-Band ESR spectrum at room temperature of $(NH_4)_2SbF_5$:MoO^{3+} with the magnetic field parallel to the *b* axis of the crystal. (b) X-Band ESR spectrum of $(NH_4)_2SbF_5$:MoO^{3+} at room temperature with the magnetic field parallel to the *a* axis of the crystal.

with the needle axis. Each antimony is at the center of an approximately octahedral configuration of ligands in which five vertices are occupied by chloride ions and one vertex is occupied by the lone pair of electrons associated with antimony in a 3+ oxidation state. Antimony ions, surrounded by four chlorine ligands (Sb–Cl_i = 2.62 Å, i = 1–4), lie in sheets with the fifth chloride (Sb–Cl_5 = 2.36 Å) either above or below the sheet. Antimony sites are equivalent, with the *b* axis parallel to the longer side of the rectangle formed by four chloride ligands and the Sb–Cl_5 axis parallel to an axis 40° from *a* in the *ac* plane. If no distortion occurs upon substitution of paramagnetic ions into antimony sites, the sites should be indistinguishable by ESR, as is observed experimentally.

ESR spectra were recorded every 10° for rotation of the single crystal about the *a*, *b*, and *c** axes. The spectra in all the crystal planes indicated the presence of only one magnetic site. ESR spectra at all the crystal orientations with respect to the applied magnetic field consisted of a central intense line corresponding to the molybdenum $I = 0$ nucleus and three relatively weak hyperfine lines on either side of the central line arising from $Mo^{95,97}$ ($I = {}^5/_2$). The measured g^2 values in each plane were least-squares fitted to eq 6 and the maximum and minimum g^2 values determined. The $\mathbf{g}^2$ tensor was diagonalized with use of Schonland's method to obtain the principal components of the **g** tensor (Table I). Since the difference between g_{xx} and g_{yy} is small (Table I), MoO^{3+} in $(NH_4)_2SbCl_5$ is, to a first approximation, an axially symmetric system. The angular variations of *g* and *A* in the crystal *bc**, *ac**, and *ab* planes were plotted and gave smooth curves with maxima for $H \| a$ and $H \| c^*$ and minima at $H \| b$. In the *ac* plane the *g* value is a maximum 40° from the *a* axis; this corresponds to $g_{zz} = g_\parallel$ and indicates that the Mo–O axis is oriented parallel to the Sb–Cl_5 direction which, in turn, is very nearly perpendicular to the plane formed by the four axial chlorides. The $A_\parallel$ and $A_\perp$ values were determined by fitting the measured g^2A^2 values from the *ac** plane to the eq 7 and are given in Table II.

$$g^2A^2 = \alpha + \beta \cos 2\theta + \gamma \sin 2\theta \quad (7)$$

The ligand hyperfine interaction, even though observed at low temperature, could not be analyzed, as all the lines were not well resolved. According to Boorman et al.,[32] the g_{av} values of $[MoOCl_4]^-$, $[MoOCl_4(H_2)]^-$, and $[MoOCl_5]^{2-}$ are 1.951, 1.947, and 1.940, respectively. Our measured g_{av} value of 1.9528 suggests that the magnetic species is $[MoOCl_4]^-$ in the present case.

Discussion

The interpretation of the ESR spin-Hamiltonian parameters of transition-metal oxohalo complexes of the type $[MOX_n]^{m-}$, where M = V, Nb, Cr, Mo, and W and X = F, Cl, Br, and I (n = 4 or 5), is generally based on the discussion of the electronic structure of vanadyl complexes by Ballhausen and Gray[33] and similar studies on chromyl and molybdenyl complexes by Gray et al.,[34,35] all based on extended Hückel calculations. For deriving expressions relating the spin-Hamiltonian parameters to the molecular orbitals of the system, it has generally been assumed that the complexes have C_{4v} symmetry with the unpaired electron in an orbital of b_2 symmetry. The molecular orbitals necessary for the discussion are then written as eq 8–10 where the ligand orbitals Φ are

$$|B_2\rangle = \beta_2|d_{xy}\rangle - \beta_2'|\Phi_{b_2}\rangle \quad (8)$$

$$|B_1\rangle = \beta_1|d_{x^2-y^2}\rangle + \beta_1'|\Phi_{b_1}\rangle \quad (9)$$

$$|E\rangle = \epsilon|d_{xz},d_{yz}\rangle - \epsilon'|\Phi_{ex},\Phi_{ey}\rangle \quad (10)$$

group orbitals of appropriate symmetry. These molecular orbitals are used to derive expressions for $g_\parallel$, $g_\perp$, $A_\parallel$, and $A_\perp$ with use of the standard second-order perturbation theory treatment of Abragam and Pryce.[36] For the transition-metal oxohalo complexes, DeArmond et al.[6] have derived the required expressions. The expressions for $g_\parallel$, $g_\perp$, $A_\parallel$, and $A_\perp$ are functions of metal and ligand spin–orbit coupling constants and $\langle r^{-3}\rangle$ values, in addition to the molecular orbital coefficients. It is customary to use these expressions to solve for

(32) P. M. Boorman, C. D. Garner, and F. E. Mabbs, *J. Chem. Soc., Dalton Trans.*, 1299 (1975).
(33) C. J. Ballhausen and H. B. Gray, *Inorg. Chem.*, **1**, 111 (1962).
(34) H. B. Gray and C. R. Hare, *Inorg. Chem.*, **2**, 363 (1962).
(35) C. R. Hare, I. Bernal, and H. B. Gray, *Inorg. Chem.*, **1**, 831 (1962).
(36) A. Abragam and M. H. L. Pryce, *Proc. R. Soc. London, Ser. A*, **205**, 135 (1961).

Table III. Spin-Hamiltonian Parameters for Vanadyl and Molybdenyl Complexes

complex	$g_\parallel$	$g_\perp$	$A_\parallel$[a]	$A_\perp$[a]	ref
$[VO(H_2O)_5]^{2+}$	1.9331	1.9813	182.8	72.0	33
$[VOF_4]^{2-}$	1.932	1.973	182.0	66.7	this work
$[VOCl_4]^{2-}$	1.9478	1.9793	168.8	62.8	21
$[VOF_5]^{3-}$	1.937	1.977	178.5	64.05	15
$[VOCl_5]^{3-}$	1.9450	1.9847	173.0	63.8	6
$[MoOF_4]^-$	1.895	1.925	85.38		this work
$[MoOCl_4]^-$	1.9650	1.9468	75.85	34.42	this work
$[MoOF_5]^{2-}$	1.874	1.911	92.93	45.13	16
$[MoOCl_5]^{2-}$	1.9632	1.940	74.7	32.6	16

[a] Hyperfine splitting constants are in $cm^{-1} \times 10^{-4}$.

the molecular orbital coefficients with use of experimental values of spin-Hamiltonian parameters and assumed values for spin–oribit coupling constants λ and $\langle r^{-3} \rangle$. Values of β_2, β_1, and ϵ obtained in this way and reported in the literature for a number of vanadyl and molybdenyl complexes are given in Table II (labeled experimental) and have been extensively used in discussing the in-plane π and σ bonding and out-of-plane π bonding in these complexes.

Values of the MO coefficients obtained in this way have been found to depend critically on the choice of λ and $\langle r^{-3} \rangle$ values. However, it has also been shown[37] that it is necessary to include contributions from occupied orbitals of b_1 symmetry to account for the observed **g**-tensor components of the chloro and bromo complexes of chromium and molybdenum. The necessary expressions have been derived,[37] but it then becomes practically impossible, without making numerous assumptions of sometimes doubtful validity, to solve for the MO coefficients from the expressions for the **g**-tensor components.

A second method for obtaining the MO coefficients is to employ quantum mechanical calculations. Semi-empirical methods such as extended Hückel theory[17,38-40] or the INDO technique[41] have been used for this purpose, but these methods provide no systematic way for reliably computing spin–orbit coupling constants and $\langle r^{-3} \rangle$ values. The MS–SCF–Xα method provides a possible way to obtain meaningful calculations of the MO coefficients, independent of experimental parameters. This method has recently been applied[37] to the series of complexes $[MOX_n]^{m-}$ (X = F, Cl, Br; M = V, Nb, Cr, Mo, W; n = 4 or 5). Both $\langle r^{-3} \rangle$ and λ values were calculated, and contributions from occupied orbitals were included. The necessary expressions for $g_\parallel$, $g_\perp$, $A_\parallel$, and $A_\perp$ in terms of the MO coefficients and other parameters were derived to allow inclusion of contributions from low-lying occupied b_1 orbitals.[37] The resulting values are given in Table II for comparison with the numbers reported in the literature from the experimental **g**- and **A**-tensor components.

The molecular orbital coefficients estimated from experimental data are larger than the values obtained from the SCF–MS–Xα method. The coefficient of the metal d_{xy} orbital β_2 in the molecular orbital containing the unpaired electron is larger for the hexacoordinated vanadium complexes than for the pentacoordinated vanadium complexes, and the reverse order is observed for molybdenum complexes (Table II). Another interesting observation is that β_2 is larger for vanadium complexes than for molybdenum complexes.

For all vanadium oxohalo complexes $g_\parallel$ is less than $g_\perp$, while $g_\parallel$ is greater than $g_\perp$ for the chloro complexes of molybdenum (Table III). There have been two proposals to account for this observation. Kon and Sharpless[9] were of the opinion that $g_\parallel$ was greater than $g_\perp$ because for chloro complexes there is more than one $^2B_1$ state which makes contribution to $g_\parallel$, while Manoharan and Rogers[16] proposed that it was the large chlorine spin–orbit coupling constant that caused this reversal of the relative magnitudes of $g_\parallel$ and $g_\perp$. Both factors appear to be of importance. From our SCF–MS–Xα studies, we conclude that the chloro complexes of molybdenum have more than one $^2B_1$ state that contributes to the $g_\parallel$ value, while for vanadium complexes only one $^2B_1$ state arising from a low-lying virtual orbital of b_1 symmetry was observed. Also, it was found necessary to take into account the ligand contributions to the **g**-tensor components to explain the observed trends.

There is only a very slight difference between the spin-Hamiltonian parameters of penta- and hexacoordinated vanadium complexes. The **A**-tensor components of the tetrafluorooxovanadium complex are larger than those of the pentafluorooxovanadium complex while for the chloro complexes the reverse is observed (Table III). For molybdenum complexes the **g**-tensor components are larger for the pentathan for the hexacoordinated complexes. The SCF–MS–Xα calculations[37] show that the fifth halide ligand does not change the orbitals necessary for computing the spin-Hamiltonian parameters of $[MOX_4]^{m-}$, or the charge on the metal, in any appreciable manner as the bonding between the metal and the axial halide ion involves only negligible metal d orbital contributions and is essentially ionic in nature.

Acknowledgment. This research was supported in part by the Department of Energy through Contract EY-76-S-02-1385.

Registry No. $[VOF_4]^-$, 78280-02-1; $[MoOCl_4]^-$, 14874-89-6; $[VOF_4]^{2-}$, 36344-83-9; $[MoOF_4]^-$, 31894-85-6; $(NH_4)_2SbF_5$, 32516-50-0; $(NH_4)_2SbCl_5$, 15221-14-4.

(37) K. K. Sunil, Ph.D. Thesis, Michigan State University, 1980; K. K. Sunil, J. F. Harrison, and M. T. Rogers, *J. Chem. Phys.*, in press.
(38) C. P. Keijzers and E. deBoer, *Mol. Phys.*, **29**, 1007 (1975).
(39) C. P. Keijzers, H. J. M. deVries, and A. van der Avoird, *Inorg. Chem.*, **11**, 1338 (1972).
(40) P. T. Manoharan and H. B. Gray, *Inorg. Chem.*, **5**, 823 (1966).
(41) S. Vijaya and P. T. Manoharan, *J. Chem. Soc., Faraday Trans. 2*, 857 (1979).